J.Natn.Sci.Foundation Sri Lanka 2023 51 (1): 113 - 127
DOI: http://dx.doi.org/10.4038/jnsfsr.v51i1.10870

RESEARCH ARTICLE

Thermal Engineering

Assessment of transverse thermal conductivity of coir fibre using experimental, analytical, and numerical methods

LG Chamath[1,3], LKT Srimal[2*] and GA Sewvandi[1]
[1] *Department of Materials Science and Engineering, Faculty of Engineering, University of Moratuwa, Moratuwa, Sri Lanka.*
[2] *Department of Mechanical and Manufacturing Engineering, Faculty of Engineering, University of Ruhuna, Hapugala, Galle, Sri Lanka.*
[3] *Division of Mechanical Engineering Technology, Institute of Technology, University of Moratuwa, Diyagama, Homagama, Sri Lanka.*

Submitted: 31 December 2021; Revised: 30 August 2022; Accepted: 23 September 2022

Abstract: Researchers aim to produce sustainable insulation materials using lignocellulose fibres (natural plant fibres). Lignocellulose fibres are readily available, biodegradable, and low-cost materials for insulation. However, these materials are formulated as composites and not as fibres alone. Thus, the thermal properties of these composites depend on the volume fraction of each phase. The evaluation of thermal conductivity can be followed by experimental, analytical, and numerical methods. Numerical and analytical methods are convenient investigational methods; they are more cost-effective, have a higher degree of flexibility in design enhancement, and are faster methods of analysing results than the experimental method. The thermal conductivity value of each phase should be used to analyse the thermal properties of composite materials. However, there is no specific method to determine the thermal conductivity of natural fibres. Therefore, this work suggests a new method to find the thermal conductivity of coir fibres. The method follows the inverse calculation of the analytical methods to find the thermal conductivity of coir fibres, and the substitution values for the equations will be determined by an experimental method. The two-phase composite was fabricated by coir fibres and epoxy with different volume fractions. Next, the thermal conductivity was measured for the fabricated composite and epoxy using the hot disk method. Finally, the transverse thermal conductivity of the fibre was calculated using available analytical models namely, the Rule of mixture, Maxwell's model, Rayleigh's model, and the Lewis-Nielsen model. The thermal conductivity value determined was 0.3058 W/mK. The results were validated through numerical modelling. The thermal conductivity of fibres was determined using a binderless compacted fibre disk, and the obtained value was 0.2797 W/mK. This value was correlated with the results obtained with the analytical and numerical methods.

Keywords: Analytical, coir, FEM, fibres, insulations, thermal conductivity.

INTRODUCTION

Energy consumption in a building is a critical factor since one-third of global energy is required for various activities in the building sector, such as cooking, lighting, air conditioning, and others (Asdrubali *et al*., 2015; Muzathik, 2016). Hence it is responsible for one-third of Green House Gas (GHG) emissions (Aditya *et al*., 2017; Kumar *et al*., 2020). Air conditioning the building to maintain indoor thermal comfort requires high energy (Katili *et al*., 2015). Therefore, reducing the cooling load for air conditioning will reduce the energy needed (Muzathik, 2003; Gunawardhana *et al*., 2016; 2017). The cooling load of the indoor atmosphere depends on the heat transfer through the building envelope (Straube, 2011). Therefore, using insulation materials will control the heat transfer through the building envelope (Aditya *et al*., 2017; Kumar *et al*., 2020).

Building insulation materials are primarily categorised as conventional materials, state-of-the-art materials, and sustainable materials (Azwa *et al*., 2013). However, many research studies are currently performed to produce insulation materials using natural plant fibres (lignocellulose fibres) (Bozsaky, 2010; Santhosh & Hiremath, 2020). The reason is that these fibres are bio-degradable, readily available, require low embodied energy for manufacturing, and are non-toxic (Manohar, 2012; Aditya *et al*., 2017; Hao *et al*., 2018). Natural

* Corresponding author (srimal@mme.ruh.ac.lk; https://orcid.org/0000-0002-3285-3214)

fibres also show properties such as low thermal conductivity, low density, and better mechanical properties. Therefore, coir fibres, oil palm fibres, sugarcane fibres, cotton, flax, hemp, and pineapple fibres are used to fabricate sustainable insulation materials (Manohar, 2012; Asdrubali *et al*., 2015; Volf *et al*., 2015; Velichko *et al*., 2017).

A binder material is necessary to adhere to these fibres without using fibre alone. Hence, these sustainable insulation materials are formulated as composite materials. The insulation properties of the composite material depend on the volume fraction of the fibres and the binder. Some research studies have investigated the effect of thermal conductivity (K_{eff}) of the composite on its fibre loading (Devireddy & Biswas, 2016; 2018; Sahu *et al*., 2016). Here, epoxy was the commonly used binder material to fabricate the composite because of its high thermal and dimensional stability, better mechanical and chemical stability, and increased durability. It also shows negligible shrinkage after the curing period due to being 100% solid phase (Saba *et al*., 2016; Yashas *et al*., 2018).

The K_{eff} of the composites were mainly analysed through experimental, analytical, and numerical methods (Devireddy & Biswas, 2016; 2018; Sunil & Manavendra, 2017; Rashid *et al*., 2019). However, analytical methods are more attractive in research as they are cheaper, faster, and more convenient than numerical and experimental methods (Sunil & Manavendra, 2017; Samarth, 2018).

Several analytical models were employed to predict the K_{eff} of the composites made from natural fibres and thermoset resins (Devireddy & Biswas, 2016; 2018; Sahu *et al*., 2016). The Rule of mixture, Maxwell's model, Rayleigh's model, and Lewis-Nielsen model helped to analyse the composites' K_{eff} (Devireddy & Biswas, 2016; 2018; Sahu *et al*., 2016). The K_{eff} of a composite can be basically calculated from the Rule of mixture. The Rule of mixture has two types of modes: parallel and series models. The parallel model can be used to determine the K_{eff} in the longitudinal direction and the series model can be used to determine the K_{eff} in the transverse direction. In the longitudinal direction, the direction of the heat flow is assumed to be parallel to the fibre orientation, and the transverse direction fibre orientation is perpendicular to the heat flow (Devireddy, 2016; Samarth, 2018). Maxwell's model is the first identified analytical model to evaluate the K_{eff} in a heterogeneous medium. Mainly it is applicable to a structure with well-distributed spherical particles in a matrix phase (Progelhof *et al*., 1976; Pietrak & Wiśniewski, 2015). This model provides accurate results up to 0.25 of volume fraction (Pietrak & Wiśniewski, 2015). Rayleigh's model is a popular model that evaluates the K_{eff} of a composite with continuous fibres. It can also be applied to mixtures with a higher volume ratio than the Maxwell model (Pietrak & Wiśniewski, 2015). Among these models, Lewis-Nielsen model is an attractive model to determine K_{eff} in transverse and longitudinal directions (Progelhof *et al*., 1976). This simple model is applicable to a wide range of filler shapes and orientations that gives higher accuracy, up to 0.4 volume fractions, without considering the interfacial thermal resistance (Pietrak & Wiśniewski, 2015).

Sahu *et al*. (2016) studied the K_{eff} for longitudinal direction in a composite made from short banana fibres and an epoxy matrix. Here, the Rule of mixture and Maxwell's and Bruggeman's models were used for analysing the results. The values obtained from the Rule of mixture show the highest deviation from the experimental results. Maxwell's and Bruggeman's results are very close to each other (Sahu *et al*., 2016). However, Bruggeman's model was developed from different assumptions than Maxwell's model, but both models were developed to evaluate the thermal conductivity in spherical particles in a continuous phase (Progelhof *et al*., 1976).

Devireddy *et al*. (2018) evaluated the K_{eff} in the longitudinal direction of a hybrid composite made from jute fibres, banana fibres, and epoxy resin. Here, the Rule of mixture, Geometric mean model, Halpin-Tsai, and Lewis-Nielsen models analytically evaluated the K_{eff}. The Geometric mean model shows the highest deviation from the experimental results. The values obtained from Halpin-Tsai and Lewis-Nielsen model show a closer relationship (Devireddy & Biswas, 2018). The Lewis-Nielsen model was obtained from the modification of the Halpin-Tsai model (Progelhof *et al*., 1976). Hence the results may have a closer relationship.

Further, Devireddy *et al*. (2016) compared the K_{eff} in the transverse direction with K_{eff} in a longitudinal direction for the hybrid composite discussed above. Here, K_{eff} values in the transverse direction produce lower values than in the longitudinal direction (Devireddy & Biswas, 2016). The reason is that the heat flux is parallel to the fibre orientation in the longitudinal arrangement, and it increases thermal conductivity (Devireddy & Biswas, 2016). Also, Mishra *et al*. (2011) evaluated the K_{eff} of the composites that contain hollow glass spheres in the epoxy matrix. Here, Maxwell's model, Russell's model, and Lewis-Nielsen model were used to evaluate K_{eff} analytically. Russell's model produced the highest deviation, and Maxwell's model offers the closest relationship with the experimental results (Mishra *et al*., 2011).

These results led to the conclusion that the analytical models' results vary with filler shape, size, distribution through the matrix, the thermal conductivity of the constituent materials, and the bond between the filler and matrix. Therefore, it is better to analyse K_{eff} of the composites using a numerical method to confirm the accuracy of the results (Pietrak & Wiśniewski, 2015; Samarth, 2018).

The above findings indicate that the thermal conductivity of each phase should be applied when analysing the K_{eff} of the composite using analytical and numerical methods. However, thermal conductivity values for these substances were obtained from the literature (Devireddy & Biswas, 2016; 2018; Sahu *et al*., 2016). The thermal conductivity of fibres has been found mainly from the binderless compacted fibre disks (Rodríguez *et al*., 2011; Manohar, 2012; Asdrubali *et al*., 2015), but the thermal conductivity value changed with the density of the fibre disk. Therefore, the thermal conductivity of a single fibre cannot be determined using this. Also, the thermal conductivity in transverse orientation is very important to design insulation materials, because the lowest thermal conductivity is given by that orientation. However, finding the transverse thermal conductivity of a single fibre is a difficult task. Therefore, this study suggests a novel method for measuring the thermal conductivity of fibres (Kumara *et al*., 2016; Chamath *et al*., 2022; Udayakumara *et al*., 2022). In the previous studies (Mishra *et al*., 2011; Devireddy & Biswas, 2016; 2018; Sahu *et al*., 2016), the K_{eff} value of the composites has been evaluated from analytical methods by substituting the thermal conductivity of each phase. For this study, the inverse calculation method is used. Here, the K_{eff} of the composite and thermal conductivity of the matrix were determined, followed by analytically defining the thermal conductivity value of fibres. With that aim, a two-phase composite was formulated with different fibre volume fractions. Here, coir fibres were selected as the fibrous material due to their low thermal conductivity (Srimal *et al*., 2014; 2015; Sathishkumar *et al*., 2018; Rashid *et al*., 2019), low density (Petroudy, 2017), and high moisture resistance (Ramamoorthy *et al*., 2015; Petroudy, 2017). Then the K_{eff} of the composite was measured experimentally, and the thermal conductivity of the coir fibres was calculated using the Rule of mixture, Maxwell model, Rayleigh's model, and Lewis-Nielsen model. The results were validated by numerical analysis.

A binderless compacted coir fibre disk was prepared, and the thermal conductivity of the disk was measured experimentally. Then the thermal conductivity of coir fibres was calculated using Landauer's equation (Smith *et al.*, 2013). The results of this method helped to validate the results of the previous method.

MATERIALS AND METHODS

Density measurement of coir fibres

Fibres were treated using a 4% NaOH solution (Chamath *et al*., 2020), and the density was measured before fabrication. The Archimedes method was used to measure the density of fibres. Here, 25 mL density bottles were used. Canola oil available in the market acted as the immersion liquid because it helps to coat the fibre well due to its low viscosity and surface tension (Truong *et al*., 2009; Amiri *et al*., 2017).

The density of fibres (ρ_{fibre}) was calculated using equation (1),

$$\rho_{fibre} = \frac{(m_2 - m_1)}{(m_4 - m_1) - (m_3 - m_2)} \times \frac{m_4 - m_1}{25} \qquad ...(1)$$

where, m_1 is the weight of the density bottle, m_2 is the weight of the density bottle with fibres, m_3 is the density bottle with canola oil and fibres, and m_4 is the weight of the density bottle with canola oil. All weighted values are given in grams (g).

Composite fabrication

The conventional hand lay-up method was used to fabricate the composite. This method is widely used in research activities due to its low cost (Elkington *et al*., 2015). However, uniaxially oriented fibres should be used to get uniform distribution in the composite (Yashas *et al*., 2018). According to Lewis-Nielsen model, if the fibre length is higher than 15 times the aspect ratio, it can be considered a uniaxially oriented fibre (Progelhof *et al*., 1976; Devireddy & Biswas, 2018). Lengthy fibres show curliness and reduce the uniaxial distribution. Because of these factors, coir fibres were cut into 5 mm in length. Then the fibres were mixed with epoxy in different volume ratios as shown in Table 1. Here, epoxy was prepared with a binder and the hardener with a 2:1 ratio according to the manufacturer's instructions. The mixture was then poured into the wooden mould (100 mm × 50 mm × 10 mm).

Table 1. Composition of fabricated samples

Sample no.	Weight of fibres (g)	Volume of epoxy (mL)	Composition
1	1.150	49.0	Fibre (2 vol%) + Epoxy (98 vol%)
2	2.300	48.0	Fibre (4 vol%) + Epoxy (96 vol%)
3	2.875	47.5	Fibre (5 vol%) + Epoxy (95 vol%)
4	4.600	46.0	Fibre (8 vol%) + Epoxy (92 vol%)
5	5.750	45.0	Fibre (10 vol%) + Epoxy (90 vol%)

The mould was allowed 48 hours to complete the curing process, and the K_{eff} of the samples were measured using the hot wire disk (Yuksel, 2016; Zhao *et al*., 2016). Each sample was cut into two separate pieces as per the instrument setup. Then the sensor of the hot wire disk was placed between the two separated samples, as shown in Figure 1. Here, the temperature of the sensor was maintained at 30 °C.

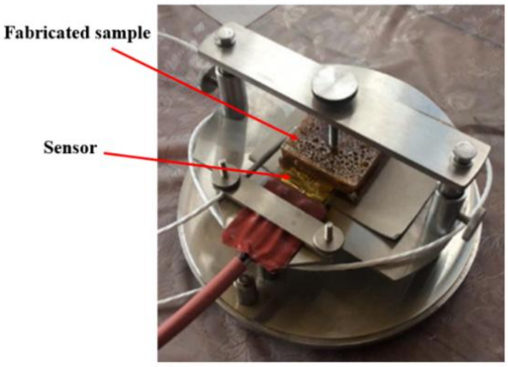

Figure 1: Measuring the thermal conductivity of the fabricated composite using the hot wire disk.

Evaluation of the thermal conductivity of fibres

The thermal conductivity of fibres was calculated from the Rule of mixture, and Maxwell's, Rayleigh's, and Lewis-Nielsen models, after measuring the K_{eff} from the hotwire disk.
Here, the fibre orientation is perpendicular to the heat flow. Therefore, a series model was necessary to analyse the K_{eff} in this orientation, as given by equation (2).

$$K_{eff} = \frac{1}{\frac{V_m}{K_m} + \frac{V_f}{K_f}} \quad \ldots(2)$$

Where K_m is the thermal conductivity of the matrix, V_m is the volume fraction of the matrix, K_f is the thermal conductivity of fibre, and V_f is the volume fraction of fibre.

Equation (3) presents Maxwell's model.

$$K_{eff} = K_m \frac{2K_m+K_f-V_f(K_m-K_f)}{2K_m+K_f+V_f(K_m-K_f)} \quad \ldots(3)$$

Equation (4) presents Rayleigh's model,

$$\frac{K_{eff}}{K_m} = 1 + \frac{2V_f}{C_1-V_f+C_2\left(0.30584{V_f}^4+0.013363{V_f}^8+\ldots\right)} \quad \ldots(4)$$

where $C_1 = \frac{K_f+K_m}{K_f-K_m}$ and $C_2 = \frac{K_f-K_m}{K_f+K_m}$.

Equation (5) presents Lewis-Nielsen model,

$$K_{eff} = K_m\left[\frac{1+ABV_f}{1-BV_f\Psi}\right] \quad \ldots(5)$$

where $B = \frac{\frac{K_f}{K_m}-1}{\frac{K_f}{K_m}+A}$ and $\Psi = 1 + \left(\frac{1-\varphi_m}{\varphi_m^2}\right)V_f$.

Table 2 presents the value of the constant 'A' in equation (5). The aspect ratio of fibre is above 15, and the direction of the heat flow is perpendicular to the direction of the fibre orientation. Therefore, 0.5 can be selected as the value for constant 'A', as per Table 2.

Table 2: The value of the constant 'A'

Type of dispersed phase	Direction of heat flow	A
Cubes	Any	2.00
Spheres	Any	1.50
Aggregate of spheres	Any	$2.50/\varphi_0$ -1
Randomly oriented rods aspect ratio = 2	Any	1.58
Randomly oriented rods aspect ratio = 4	Any	2.08
Randomly oriented rods aspect ratio = 6	Any	2.80
Randomly oriented rods aspect ratio = 10	Any	4.93
Randomly oriented rods aspect ratio = 15	Any	8.38
Uniaxial oriented fibres	Parallel to fibres	$2L/D$
Uniaxial oriented fibres	Perpendicular to fibres	0.50

Table 3 provides the value of constant 'φ_m'. The fibre distribution is uniaxial random. Therefore, the value of 0.8200 could be selected as the φ_m value.

Finite element method

It is better to validate the analytically evaluated thermal conductivity value using a numerical method. Normally, fibres are randomly distributed throughout the matrix in a composite; hence it is difficult to model the random arrangement in the numerical method. However, the main objective of the research is the evaluation of the transverse thermal conductivity of the fibres. Therefore, the heat flow should be applied perpendicular to the fibre direction. Also, some assumptions are considered during the computational analysis, such as, fibres and matrix are microscopically and homogeneously distributed throughout the composite, fibres have the same shape and size, fibre and matrix have a perfect bonding, thermal resistance between two phases is negligible, and the composite is void-free throughout (Rao *et al*., 2015; 2018; Priya *et al*., 2016; Devireddy & Biswas, 2018;

Rashid *et al*., 2019). The Ansys software package was used for this study while considering the abovementioned assumptions (Sahu *et al*., 2016; Sunil, 2017; Devireddy & Biswas, 2018; Rashid *et al*., 2019).

Table 3: The value of constant 'φ_m'

Shape of particle	Type of packing	φ_m
Spheres	Hexagonal close	0.7405
Spheres	Face centred cubic	0.7405
Spheres	Body centred cubic	0.6000
Spheres	Simple cubic	0.5240
Spheres	Random close	0.6370
Spheres	Random close	0.6010
Rods of fibres	Uniaxial hexagonal close	0.9070
Rods of fibres	Uniaxial simple cubic	0.7850
Rods of fibres	Uniaxial random	0.8200
Rods of fibres	Three-dimensional random	0.5200

Also, it is important to identify the cross-section view of the coir fibre to decide the element for the numerical analysis. Therefore, scanning electron microscope (SEM) image analysis was done to obtain a cross-section view of the fibres. The fibres have an approximately circular cross-section, as shown in Figure 2. The circular cross-section provides an additional advantage for the analytical and numerical modelling of the composite.

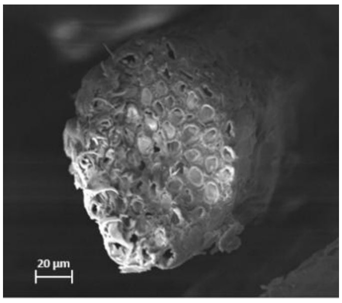

Figure 2: SEM image representing the cross-section of a coir fibre (×1000)

Then, the fibre distribution in the epoxy matrix could be assumed as a square pattern and hexagonal pattern, as shown in Figure 3 for the numerical analysis (Sihn & Roy, 2011; Rao *et al*., 2015; Devireddy & Biswas, 2016).

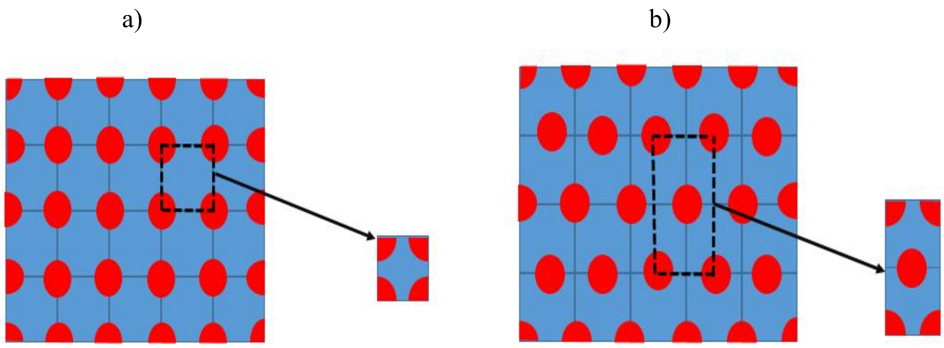

Figure 3: Schemic representation of the fibre distribution in a) square pattern, b) hexagonal pattern

Then, the fibre distribution can be simplified as an isolated unit cell that has a three-dimensional physical model with a periodic arrangement of cylindrical fibres in epoxy cubes. Figure 4 represents the isolated unit cell of the square array pattern (Sahu *et al*., 2016; Devireddy & Biswas, 2018).

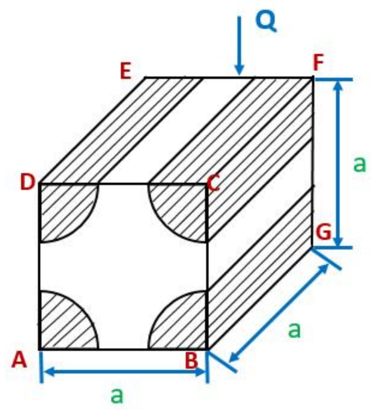

Figure 4: Isolated unit cell of the square array pattern

The above unit cells are simplified as a quarter unit cell, as shown in Figure 5, to reduce the complexity of geometry and computing time (Rao *et al*., 2015). It is vital to use an orthogonal coordinate system that represents the fibre direction on the z-axis; the x-axis is the plane of the unit cell, which is perpendicular to the fibres, and the y-axis is perpendicular to the plane of the unit cell and perpendicular to the fibres. Here, the fibre diameter was measured using a primo star iLED microscope, and the average diameter was 201.6 µm, while the length of the unit cell was calculated corresponding to the volume ratio of 0% to 0.1%.

(a) (b)

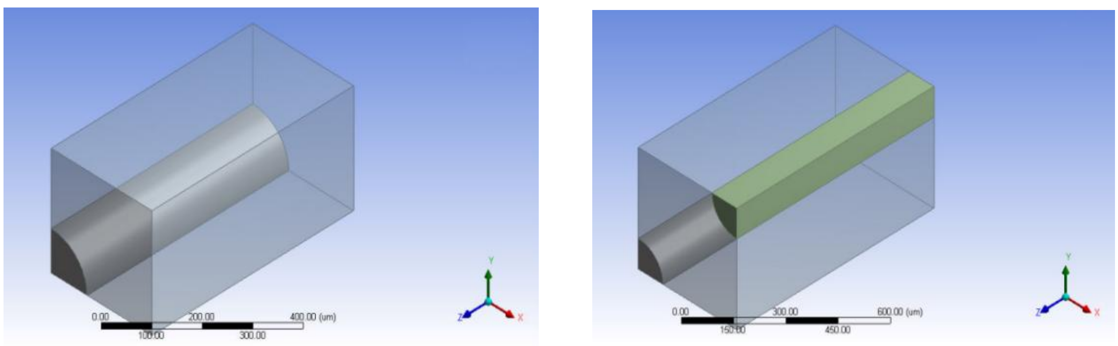

Figure 5: The developed quarter unit cell for the numerical analysis a) square array, b) hexagonal array

The boundary condition for FEM to analyse thermal conductivity

For finding the transverse thermal conductivity of the unit cell, the heat load was applied as a temperature for both plane face (30 °C) and opposite face (25 °C) to maintain a temperature difference of 5 °C. Other faces, parallel to the heat flow, are assumed to be adiabatic (Ilyas & Rejeesh, 2015; Priya *et al*., 2016; Devireddy & Biswas, 2018; Rao, 2018). The heat distribution throughout the unit cell was analysed by Ansys software, and the thermal conductivity of the unit cell was calculated by Fourier's law, as shown in equation (6),

$$Q_x = -K\,(dT/da) \qquad \text{...(6)}$$

where K is the thermal conductivity of the unit cell, dT/da is the temperature gradient in the x-direction, and Q_x is the heat flux along the x-direction.

Preparation of coir fibre specimen to measure thermal conductivity

A cylindrical-shaped specimen was prepared by compressing 5 mm coir fibres without using a binder (Rodríguez *et al*., 2011). Here, a 20 Mpa pressure was applied on 6.61 g coir fibres with a mould diameter of 25 mm. The thermal conductivity reading was obtained from the hot wire disk after removing the specimen from the mould, as shown in Figure 6.

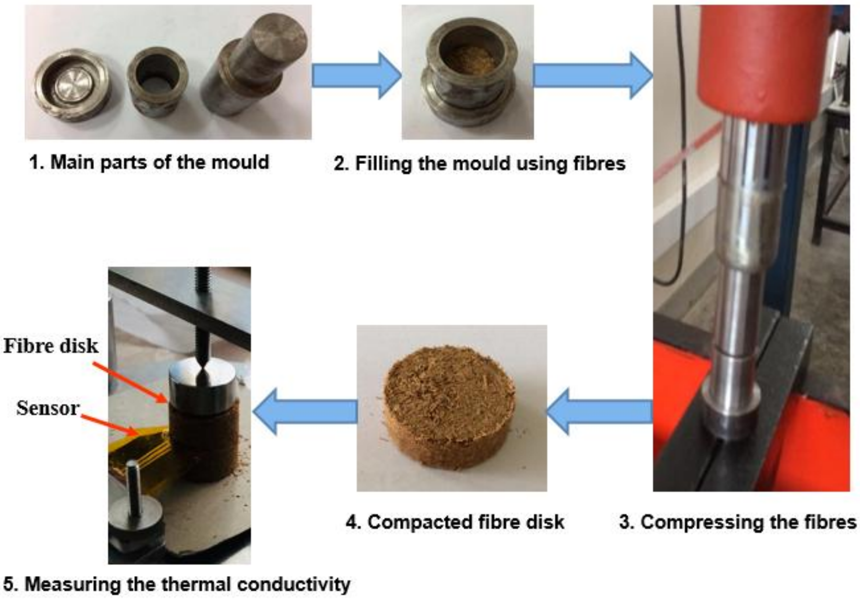

Figure 6: Illustration of the preparation method of binder-less compacted disk

Then the density of the compacted disk was calculated, and it was 0.936 gcm^{-3}. According to this density value, the compacted fibre disk contains a 0.2280 volume fraction of air. However, to predict the thermal conductivity of coir fibres, Landauer's equation was used to calculate the thermal conductivity of coir fibres because the structure is open porous when the volume fraction is in the range of $0.15 < Vp < 0.65$ (Smith *et al*., 2013). Equation (7) provides the Landauer's equation.

$$K_{eff} = \frac{1}{4}\left[K_p(3V_p - 1) + K_m(2 - 3V_p) + \left\{\left[K_p(3V_p - 1) + K_s(2 - 3V_p)\right]^2 + 8K_mK_p\right\}^{1/2}\right] \quad \dots (7)$$

Where K_p is the thermal conductivity of air at 25 °C, and V_p is the volume fraction of air.

RESULTS AND DISCUSSION

Thermal conductivity of the fabricated composite

A significant influence is noted in the effective thermal conductivity of the composite after adding fibres. The K_{eff} of the composites increases with fibre loading. It was concluded that the thermal conductivity of fibre is higher than the thermal conductivity of pure epoxy.

The transverse K_{eff} of the composite for each fibre loading and the thermal conductivity value of epoxy were substituted to the Rule of mixture, and Maxwell's, Rayleigh's, and Lewis Nielsen's models, to find the fibre thermal conductivity. Table 4 summarises the calculated thermal conductivity values of fibres for each loading.

Figure 7 illustrates the measured K_{eff} of the composites with different fibre loadings of coir fibre in the transverse direction using the hot wire disk.

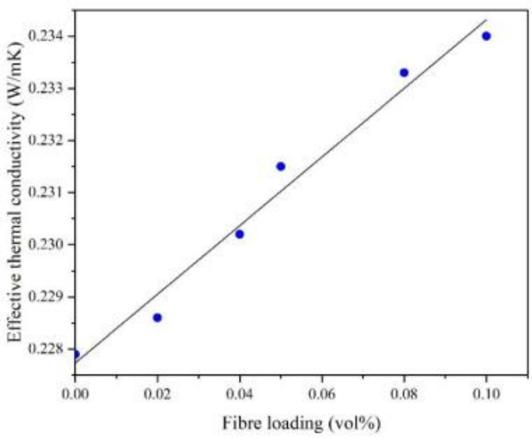

Figure 7: Effective thermal conductivity of the fabricated composites using the hot wire disk

Table 4: Calculation of thermal conductivity of coir fibre

Fibre loading	K_{eff} of the composite	K_f from Rule of mixture	K_f from Maxwell's model	K_f from Rayleigh's model	K_f from Lewis-Nielsen model
0.02	0.2286	0.2946	0.2815	0.2836	0.2825
0.04	0.2302	0.3172	0.2992	0.3029	0.3049
0.05	0.2315	0.3432	0.3140	0.3199	0.3249
0.08	0.2333	0.3209	0.2960	0.2999	0.3138
0.10	0.2340	0.3133	0.2976	0.3015	0.3028
Average K_f value		0.3192	0.2977	0.3016	0.3058

According to the above calculation, the average K_f values obtained from different models are 0.3192 W/mK, 0.2977 W/mK, 0.3016 W/mK, and 0.3058 W/mK.

Selecting the most suitable value is challenging. Hence, each value is separately substituted to the Rule of mixture, and Maxwell's, Rayleigh, and Lewis Nielsen models. The behaviour of substituted values in the models was then compared with the experimental values to select the best value for the K_f. Figures 8 a), b), c) and d) present the comparisons of the substituted values into models with experimental values

The models show a variation with the regression line of the experimental values according to Figures 8a) – 8d). The reason is the difference in the assumption during the development of micromechanical models of the analytical models, such as fibre shape, distribution, and interfacial contact between the matrix and fibre material. Also, void formation in the composite and changes in the orientation of fibres may have caused this situation. Therefore, it is essential to calculate percentage errors associated with the respective experimental values with models to identify the best value for K_f.

Table 5 presents the percentage errors associated with the respective experimental values with the substituted K_f value of 0.3192 W/mK to the Rule of mixture and Maxwell's, Rayleigh's, and Lewis Nielsen's models in Figure 8a).

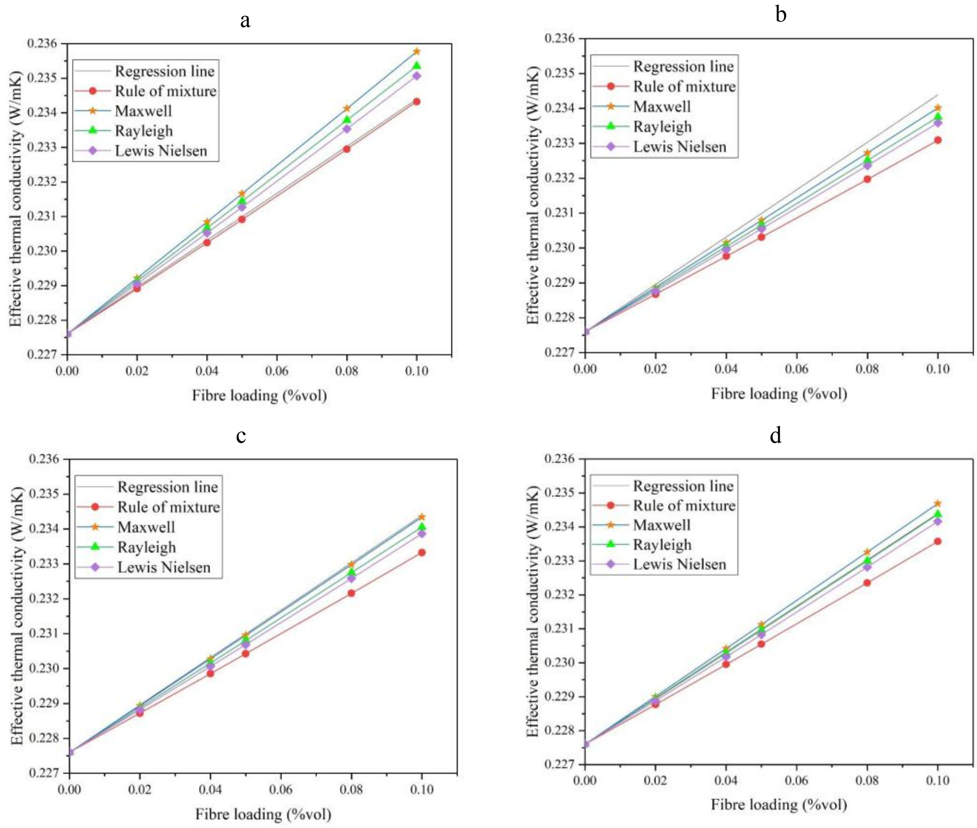

Figure 8: The behaviour of thermal conductivity of fibre with analytical models a) thermal conductivity value 0.3192 W/mK; b) thermal conductivity value 0.2977 W/mK; c) thermal conductivity value 0.3016; W/mK d) thermal conductivity value 0.3058 W/mK

Table 5: Percentage errors in Figure 8a) with the experimental values

Fibre Loading	Experimental K_{eff} (W/mK)	Percentage error			
		Rule of mixture	Maxwell	Rayleigh	Lewis Nielsen
0.02	0.2290	0.0218	0.1136	0.0742	0.0393
0.04	0.2303	0.0347	0.2301	0.1520	0.0912
0.05	0.2340	0.0390	0.2857	0.1905	0.1169
0.08	0.2330	0.0343	0.4678	0.3218	0.2189
0.10	0.2343	0.0299	0.5888	0.4138	0.2901
Average percentage error (E)		0.0319	0.3372	0.2305	0.1513
Mean value of E		0.1877			

The Rule of mixture and Maxwell's, Rayleigh's, and Lewis-Nielsen models give the average percentage errors (E) of 0.0319, 0.3372, 0.2305, and 0.1513, respectively. The mean value of E is 0.1877. The same calculations were made for Figures 8b) -8d), and the results are summarised in Table 6.

Table 6. Mean value of E in Figures 8a) – 8d)

Figure No.	Substituted K_f value (W/mK)	Mean value of E
8a)	0.3192	0.1877
8b)	0.2977	0.2029
8c)	0.3016	0.1321
8d)	0.3058	0.0923

The substitution of the K_f value of 0.3058 W/mK produced a minimum percentage error of 0.0923. Therefore, the thermal conductivity of coir fibre can be taken as 0.3058 W/mK. It is important to validate this value using a numerical method, and the next section discusses the numerical analysis for the validation.

Numerically validating the thermal conductivity of fibres

The value of 0.3058 W/mK was validated from the numerical methods using square array pattern and hexagonal array pattern. Figure 9 provides the temperature distribution in square and hexagonal array patterns for the 0.1 fibre ratio.

a) (b)

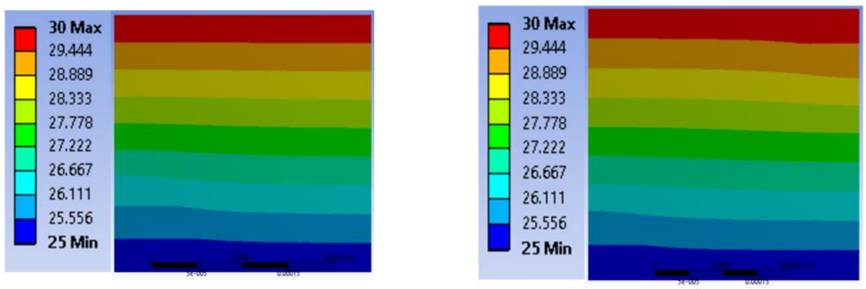

Figure 9: The temperature distribution in quarter unit cell: a) square array pattern, b) hexagonal array pattern

The temperature distribution is uniform in the upper region of Figure 9a). However, it shows an uneven distribution around the bottom region of the quarter unit cell due to the presence of fibre. Also, the temperature distribution is uneven in the top and bottom regions of Figure 9b) due to the presence of fibres. But it will show a uniform distribution in the middle region of the quarter unit cell.

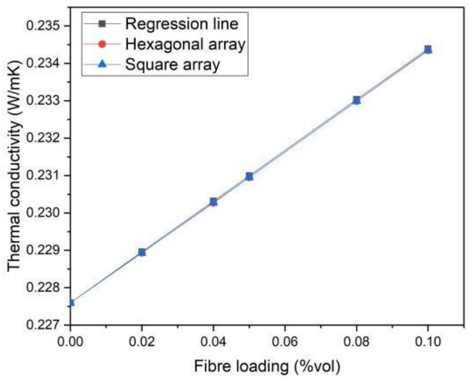

Figure 10: Comparison of the thermal conductivity values from the experimental and numerical methods

According to Figure 10, the values obtained from the numerical method overlap with the regression line of the experimental values. Hence, the transverse thermal conductivity of the coir fibres can be accepted as 0.3058 W/mK according to the results of experimental, analytical, and numerical methods.

Thermal conductivity of compacted coir fibres

According to the cross-section view of the SEM image analysis in Figure 2, fibres show a porous structure. However, the thermal conductivity of the fibre is given by the combination of the porous and cellulose parts, because the porous structure is not continuous from one end to another end of the fibre. This porous structure is given by the lumen of the fibre cell structure. Therefore, it can be assumed as a close porous structure. In the composite fabrication method, the fibre surface was fully covered by epoxy. Therefore, in the binderless compacted disk method Landauer's method should be applied to the whole structure of the fibre, with a combination of porous and cellulose parts due to the close porosity of the fibre.

According to Landauer's method in equation (7), the calculated value of the thermal conductivity of coir fibres is 0.2797 W/mK. The results obtained from the compacted fibre disk are close to the value of 0.3058 W/mK. However, the variation in the results may be due to the interfacial thermal resistance in the structure (Ahmadi *et al*., 2019).

CONCLUSION

In this study, a composite material was fabricated using epoxy and coir fibres for different fibre loadings. Then the effective thermal conductivity (K_{eff}) of the composites was measured. Here, the K_{eff} of the composite was higher than the thermal conductivity of pure epoxy, and the K_{eff} was increased with the increasing fibre loading in the composite. Hence, it may be due to the higher thermal conductivity of coir fibres than epoxy. Then the experimentally measured K_{eff} values can be used to calculate the thermal conductivity of coir fibres analytically. Therefore, the analytical models are a practical approach to finding the thermal conductivity in coir fibres due to the close relation with the experimental values. The transverse thermal conductivity of the fibre could be taken as 0.3058 W/mK by the comparison of the results obtained from the analytical models. Additionally, validation of the transverse thermal conductivity value of 0.3058 W/mK using the numerical method will add value to this research work. Here, the numerical results and experimental results overlapped with each other and it proved that 0.3058 W/mK could be taken as the thermal conductivity of the fibre. Further, a binderless compacted fibre disk was prepared and the thermal conductivity of the disk was measured to validate the results obtained from the previous method. Here, the void content of the disk was 22.8%, which shows an open porous structure. Therefore, the thermal conductivity of fibre was calculated using Landauer's equation and the value was 0.2797 W/mK. However, this method could be used to validate the value of 0.3058 W/mK, despite the difference between the two values.

Acknowledgement

The authors wish to thank the Department of Physics, The Open University Sri Lanka and Department of the Mechanical Engineering, University of Moratuwa, Sri Lanka for providing valuable support in the resource arrangements of this study.

REFERENCES

Aditya L., Mahlia T.M.I., Rismanchi B., Ng H.M., Hasan M.H., Metselaar H.S.C., Muraza O. & Aditiya H.B. (2017). A review on insulation materials for energy conservation in buildings. *Renewable and Sustainable Energy Reviews* **73**: 1352–1365.
DOI: https://doi.org/10.1016/j.rser.2017.02.034

Ahmadi M., Ansari R. & Hassanzadeh-Aghdam M.K. (2019). Finite element analysis of thermal conductivities of unidirectional multiphase composites. *Composite Interfaces* **26**(12): 1035–1055.
DOI: https://doi.org/10.1080/09276440.2019.1578588

Amiri A., Triplett Z., Moreira A., Brezinka N., Alcock M. & Ulven C.A. (2017). Standard density measurement method development for flax fiber. *Industrial Crops and Products* **96**: 196–202.
DOI: https://doi.org/10.1016/j.indcrop.2016.11.060

Asdrubali F., D'Alessandro F. & Schiavoni S. (2015). A review of unconventional sustainable building insulation materials. *Sustainable Materials and Technologies* **4**: 1–17.
DOI: https://doi.org/10.1016/j.susmat.2015.05.002

Azwa Z.N., Yousif B.F., Manalo A.C. & Karunasena W. (2013). A review on the degradability of polymeric composites based on natural fibres. *Materials and Design* **47**: 424–442.
DOI: https://doi.org/10.1016/j.matdes.2012.11.025

Bozsaky D. (2010). The historical development of thermal insulation materials. *Periodica Polytechnica Architecture* **41**(2): 49–56.
DOI: https://doi.org/10.3311/pp.ar.2010-2.02

Chamath L.G., Srimal L.K.T. & Sewvandi G.A. (2020). Effect of alkaline concentration on the surface properties of coir fibers. *Proceeding of the National Engineering Research Symposium*, volume 1, 10 December. NERDC, Ja Ela, Sri Lanka, pp. 7–12.
DOI: 10.13140/RG.2.2.36167.37283

Chamath L.G., Srimal L.K.T. & Sewvandi G.A. (2022). Evaluating the thermal conductivity of three-phase insulation

composite using analytical and numerical methods. *2022 Moratuwa Engineering Research Conference (MERCon)*, 27–29 July. University of Moratuwa, Sri Lanka.
DOI: 10.1109/MERCon55799.2022.9906166

Devireddy S.B.R. & Biswas S. (2016). Physical and thermal properties of unidirectional banana-jute hybrid fiber-reinforced epoxy composites. *Journal of Reinforced Plastics and Composites*. **35**(15): 1157–1172.
DOI: https://doi.org/10.1177/0731684416642877

Devireddy S.B.R. (2016). Mechanical, thermal and physical properties of hybrid banana-jute fibers reinforced epoxy and polyester composites : modeling and experiments mechanical, thermal and physical properties of hybrid banana-jute fibers reinforced epoxy and polyester. *PhD Thesis*, National Institute of Technology, Rourkela, India.

Devireddy S.B.R. & Biswas S. (2018). Thermo-physical properties of short banana–jute fiber-reinforced epoxy-based hybrid composites. *Proceedings of the Institution of Mechanical Engineers, Part L: Journal of Materials: Design and Applications* **232**(11): 939–951.
DOI: https://doi.org/10.1177/1464420716656883

Elkington M., Bloom D., Ward C., Chatzimichali A. & Potter K. (2015). Hand layup: understanding the manual process. *Advanced Manufacturing: Polymer and Composites Science* **1**(3): 138–151.
DOI: https://doi.org/10.1080/20550340.2015.1114801

Gunawardhana H.P.B., Chamath L.G. & Sewvandi G. A. (2016). A methodology to control the interior temperature of vehicles parked under the sun. *Proceeding of the 2016 Manufacturing and Industrial Engineering Symposium (MIES)*, 22–22 October. Waters Edge, Battaramulla, Sri Lanka, pp. 1–5.
DOI: https://doi.org/10.1109/MIES.2016.7779990

Gunawardhana H.P.B., Chamath L.G. & Sewvandi G.A. (2017). Solar powered mini air conditioner for automobiles. *Proceeding of the Materials Engineering Symposium on Innovations for Industry*, Department of Materials Science and Engineering, University of Moratuwa, Sri Lanka. Available at *http://dl.lib.uom.lk/handle/123/17361*, Accessed 27 August 2022.

Hao L.C., Sapuan S.M., Hassan M.R. & Sheltami R.M. (2018). Natural fiber reinforced vinyl polymer composites. In: *Natural Fibre Reinforced Vinyl Ester and Vinyl Polymer Composites*, pp 27–70. Woodhead Publishing, Sawston, UK.
DOI: https://doi.org/10.1016/b978-0-08-102160-6.00002-0

Ilyas N.P. & Rejeesh C.R. (2015). Modelling and thermal analysis of medium density coir composite boards. *International Journal of Engineering Research and Technology* **4**(08): 557–559.
DOI: https://doi.org/10.17577/IJERTV4IS080554

Katili A.R., Boukhanouf R. & Wilson R. (2015). Space cooling in buildings in hot and humid climates - a review of the effect of humidity on the applicability of existing cooling techniques. *Proceedings of 14th International Conference on Sustainable Energy Technologies (SET)*, 25–27 August, Nottingham, UK.
DOI: https://doi.org/10.13140/RG.2.1.3011.5287

Kumar D., Alam M., Zou P.X.W., Sanjayan J.G. & Memon R.A. (2020). Comparative analysis of building insulation material properties and performance. *Renewable and Sustainable Energy Reviews* **131**: 110038.
DOI: https://doi.org/10.1016/j.rser.2020.110038

Kumara P.D.C., Viraj M.P.S., Jayaweera H.H.E., Muzathik A.M. & Ariyaratne T.R. (2016). Experimental investigation of the temperature dependency of the thermal conductivity of glass wool used in a steam generator. *Proceedings of the Annual Research Symposium 2016*, 11–22 October. University of Colombo, Sri Lanka, p. 275.

Manohar K. (2012). Experimental investigation of building thermal insulation from agricultural by-products. *British Journal of Applied Science and Technology* **2**(3): 227–239.
DOI: https://doi.org/10.9734/bjast/2012/1528

Mishra D., Satapathy A. & Patnaik A. (2011). Processing and thermal conductivity characterization of solid glass micro-spheres filled polymer composites. *Proceeding of 14th International Conference on Advanced Materials and Processing Technologies*, Istanbul, Turkey.

Muzathik A.M. (2003). Economic potential of energy conservation in a five star hotel. *M.Eng. thesis*, University of Moratuwa, Sri Lanka. Available at *http://dl.lib.mrt.ac.lk/theses/handle/123/401*, Accessed 27 August 2022.

Muzathik A.M. (2016). Green Sri Lanka through energy conservation: commercial building as a case study. The Official e-newsletter of the Institution of Engineers Sri Lanka. Available at *http://ioes18.wildapricot.org/Green-Sri-Lanka-through-energy-conservation*, Accessed 27 August 2022.

Petroudy S.R.D (2017). Physical and mechanical properties of natural fibers. In: *Advanced High Strength Natural Fibre Composites in Construction*, pp. 59–83. Woodhead Publishing, Sawston, UK.
DOI: https://doi.org/10.1016/B978-0-08-100411-1.00003-0

Pietrak K. & Wiśniewski T. (2015). A review of models for effective thermal conductivity of composite materials. *Journal of Power of Technologies* **95**(1): 1424.

Priya K.B., Abid A.M. & Sai R.N.G. (2016). Design and analysis of square model unit cell for the prediction of thermal conductivity of fibre reinforced composites. *International Journal of Applied Engineering Research* **11**(10): 7166–7170.

Progelhof R.C., Throne J.L. & Ruetsch R.R. (1976). Methods for predicting the thermal conductivity of composite systems:

A review. *Polymer Engineering and Science* **16**(9): 615–625.
DOI: https://doi.org/10.1002/pen.760160905

Rao B.R., Raju V.R. & Rao K.M. (2015). Effect of fibre shape on transverse thermal conductivity of unidirectional composites. *Sadhana - Academy Proceedings in Engineering Sciences* **40**(2): 503–513.
DOI: https://doi.org/10.1007/s12046-014-0323-9

Ramamoorthy S.K., Skrifvars M. & Persson A. (2015). A review of natural fibers used in biocomposites: Plant, animal and regenerated cellulose fibers. *Polymer Reviews* **55**(1): 107–162.
DOI: https://doi.org/10.1080/15583724.2014.971124

Rao T.S., Rao B.R. & Murthy V.B. (2018). Transverse thermal conductivity of hollow fiber composites. *International Journal of Engineering Technology Science and Research* **5**(5): 389–394.

Rashid K., Haq E.U., Kamran M.S., Munir N., Shahid A. & Hanif I. (2019). Experimental and finite element analysis on thermal conductivity of burnt clay bricks reinforced with fibers. *Construction and Building Materials* **221**: 190–199.
DOI: https://doi.org/10.1016/j.conbuildmat.2019.06.055

Rodríguez N.J., Yáñez-Limón M., Gutiérrez-Miceli F.A., Gomez-Guzman O., Matadamas-Ortiz T.P., Lagunez-Rivera L. & Feijoo J.A.V. (2011). Assessment of coconut fibre insulation characteristics and its use to modulate temperatures in concrete slabs with the aid of a finite element methodology. *Energy and Buildings* **43**(6): 1264–1272.
DOI: https://doi.org/10.1016/j.enbuild.2011.01.005

Saba N., Jawaid M., Alothman O.Y., Paridah M.T. & Hassan A. (2016). Recent advances in epoxy resin, natural fiber-reinforced epoxy composites and their applications. *Journal of Reinforced Plastics and Composites* **35**(6): 447–470.
DOI: https://doi.org/10.1177/0731684415618459

Sahu Y.K., Agrawal A. & Satapathy A. (2016). Heat conduction behavior of short fiber reinforced polymer composites. *International Journal of Advanced Technology in Engineering Science* **4**(1): 215–226.

Samarth S. (2018). Effective thermal conductivity of polymer composites: a review of analytical methods. *International Journal of Ambient Energy* **42**(8): 961–972.
DOI: https://doi.org/10.1080/01430750.2018.1557544

Santhosh S.K. & Hiremath S.S. (2020). Natural fiber reinforced composites in the context of biodegradability: A review. *Encyclopedia of Renewable and Sustainable Materials* **5**(2020): 160–178.
DOI: https://doi.org/10.1016/b978-0-12-803581-8.11418-3

Sathishkumar S., Naveen T.K., Jeevarathinam A., Karthik V. & Dhandapani N.V. (2018). Thermal conductivity of natural fiber reinforced plastics. *International Journal of Pure and Applied Mathematics* **118**(20): 43–51.

Sihn S. & Roy A.K. (2011). Micromechanical analysis for transverse thermal conductivity of composites. *Journal of Composite Materials* **45**(11): 1245–1255.
DOI: https://doi.org/10.1177/0021998310382311

Smith D.S., Alzina A., Bourret J., Nait-Ali B., Pennec F., Tessier-Doyen N., Otsu K., Matsubara H., Elser P. & Gonzenbach U.T. (2013). Thermal conductivity of porous materials. *Journal of Materials Research* **28**(17): 2260–2272.
DOI: https://doi.org/10.1557/jmr.2013.179

Srimal L.K.T., Fernando M.A.R.V. & Sumith B. (2014). Value addition for coir fiber as low temperature insulation material. *MSc Thesis*. University of Moratuwa, Sri Lanka. Available at *http://dl.lib.uom.lk/handle/123/10957*, Accessed 27 August 2022.

Srimal L.K.T. & Sumith B. (2015). Value addition for coir fiber as low temperature insulation material. *Proceeding of the 12th Academic Sessions 2015*, 4 March. University of Ruhuna, Matara, Sri Lanka.

Straube J. (2011) Thermal controls in building, *Building Science Corporation*. Available at *www.buildingscience.com/documents/digests/bsd-011-thermal-control-in-buildings*, Accessed 27 August 2022.

Sunil E.M. & Manavendra G. (2017). Experimental investigation on thermal properties of bagasse fly ash reinforced epoxy composite. *International Research Journal of Engineering and Technology* **4**(4): 124–128.
DOI: https://doi.org/10.13140/RG.2.2.25891.32808

Truong M., Zhong W., Boyko S. & Alcock M. (2009). A comparative study on natural fibre density measurement. *Journal of the Textile Institute* **100**(6): 525–529.
DOI: https://doi.org/10.1080/00405000801997595

Udayakumara D.G.G.V., De Silva I.R., Chamath L.G., Srimal L.K.T. & Gallage R. (2022). Design and fabrication of a system to measure thermal conductivity of compressible materials. *Proceeding of the 19th Academic Sessions 2022, University of Ruhuna, Matara, Sri Lanka.* Available at *http://ir.lib.ruh.ac.lk/xmlui/handle/iruor/5788*, Accessed 27 August 2022.

Velichko E., Tskhovrebov E. & Shevchenko A. (2017). Environmental safety providing during heat insulation works and using thermal insulation materials. *MATEC Web of Conferences* **106**: 03009.
DOI: https://doi.org/10.1051/matecconf/201710603009

Volf M., Diviš J. & Havlík F. (2015). Thermal, moisture and biological behaviour of natural insulating materials. *Energy Procedia* **78**: 1599–1604.
DOI: https://doi.org/10.1016/j.egypro.2015.11.219

Yashas G.T.G., Sanjay M.R., Subrahmanya B.K., Madhu P., Senthamaraikannan P. & Yogesha B. (2018). Polymer matrix-natural fiber composites: an overview. *Cogent Engineering* **5**(1): 1446667.

DOI: https://doi.org/10.1080/23311916.2018.1446667
Yuksel N. (2016). The review of some commonly used methods and techniques to measure the thermal conductivity of insulation materials. In: *Insulation Materials in Context of Sustainability,* pp. 113–140. IntechOpen, London, UK,
Zhao D., Qian X., Gu X., Jajja S.A. & Yang R. (2016). Measurement techniques for thermal conductivity and interfacial thermal conductance of bulk and thin film materials. *Journal of Electronic Packaging, Transactions of the ASME* **138**(4): 1–64.
DOI: https://doi.org/10.1115/1.4034605